Influence of heat treatment on crystallization of strontium barium niobate (SBN) ferroelectric thin films

1999 J. Phys.: Condens. Matter 11 9611

(http://iopscience.iop.org/0953-8984/11/48/318)

J. Phys.: Condens. Matter **11** (1999) 9611–9617. Printed in the UK PII: S0953-8984(99)07800-5

Influence of heat treatment on crystallization of strontium barium niobate (SBN) ferroelectric thin films

R G Mendes, E B Araújo† and J A Eiras

Universidade Federal de São Carlos, Departamento de Física, Grupo de Cerâmicas Ferroelétricas, Caixa Postal 676, 13565-670 São Carlos SP, Brazil

Received 14 September 1999

Abstract. Strontium barium niobate (SBN) thin films of good quality were deposited on Si and Pt/Si substrates using a polymeric resin containing metallic ions. Using x-ray diffraction, the presence of SBN phase for films annealed at 600 °C and 700 °C for 1 hour was identified on both substrates. Films were also crystallized by rapid thermal annealing (RTA) at different temperatures and for different times, presenting good crystallization. Undesired phases such as $SrNb_2O_6$ and $BaNb_2O_6$ appear in films deposited on Si and Pt/Si substrates for films crystallized using a conventional furnace. However, using RTA these phases were eliminated for films annealed at 700 °C for 60 and 120 seconds.

1. Introduction

The tungsten bronze family is one of several ferroelectric materials. Since 1949, when the tungsten bronze structure was deduced by Magneli [1], numerous tungsten bronzes have been synthesized. The tungsten bronze family includes niobates such as (Sr,Ba)Nb_2O_6 (SBN), (Pb,Ba)Nb_2O_6 (PBN) and (Pb,K)Nb_2O_6 (PKN). PBN and PKN have orthorhombic tungsten bronze structure with point group $mm2$. On the other hand, SBN ($Sr_xBa_{1-x}Nb_2O_6$) presents a tetragonal or orthorhombic phase, depending on composition and temperature. A solid solution of SBN exists in the binary $SrNb_2O_6$–$BaNb_2O_6$ system. Investigations using x-ray diffraction suggested a morphotropic phase boundary (MPB) around $x = 0.25$, which is characterized by the coexistence of the tetragonal and orthorhombic phases [2]. SBN with $x = 0.2$ presents a tetragonal ferroelectric phase between 120 and 293 °C; below 120 °C it presents an orthorhombic phase and a tetragonal paraelectric phase above 293 °C. The tetragonal SBN structure consists of a framework of NbO_6 octahedra sharing corners in such a way that three types of interstitial site result.

Figure 1 shows a view of the SBN structure along the polar axis presented by Jamieson *et al* [3]. Niobium atoms occupy the B1 and B2 sites in this structure. The strontium atom in the A1 site has 12 nearest oxygen atoms in distorted cubo-octahedral coordination while the barium/strontium atom in the A2 site is surrounded by nine nearest-neighbour oxygen atoms and this arrangement may be described as in distorted tricapped trigonal prismatic coordination [3]. The structure devised by Jamieson *et al* is still accepted for SBN, although there has always been some question as to whether or not barium is found only on the A2 site. Recent investigations show that barium is found only at the A2 site while strontium occupies the A1 and A2 sites [4].

† Author to whom correspondence should be addressed.

0953-8984/99/489611+07$30.00

The excellent ferroelectric and electro-optic properties exhibited by SBN make this material promising for a variety of applications. SBN has received great attention as a ferroelectric material due to its large pyroelectric coefficient [5], piezoelectric [6] and electro-optic properties [7, 8].

In recent years, the development of integrated optical devices has stimulated the demand for thin films using attractive materials such as SBN. SBN thin films have been prepared by several techniques like sol–gel processing [9, 10], pulsed laser deposition [11, 12] and metallorganic chemical vapour deposition (MOCVD) [13, 14]. Large-scale processing of high-quality thin films requires low-temperature synthesis, high reproducibility and simplicity in all processing steps at low cost. Due to this fact, the search for new routes for film preparation remains an interesting and open subject in order to improve the stability of complex solutions, the control of the stoichiometry of the film composition or to reduce the cost of the process. Very recently, the preparation of SBN thin films by a chemical method based on a polymeric resin containing metallic ions was proposed [15]. The method was successfully applied to prepare SBN thin films on Si or Pt/Si substrates to obtain films of good quality and homogeneity.

In this work, SBN thin films obtained by the above-cited method were studied regarding their structural properties. The effect of different heat treatments on SBN thin films, using a conventional furnace and rapid thermal annealing (RTA), was studied using x-ray diffraction at room temperature.

2. Experimental procedure

In this work SBN films were prepared by a hybrid chemical method, used to produce a polymeric resin [15]. The general idea is to distribute the metallic ions homogeneously throughout the polymeric resin, prepared according to the Pechini method [16, 17]. The process calls for forming a chelate between dissolved ions with a hydroxycarboxylic acid (citric acid). Heating of the resin in air causes a breakdown of the polymer. Subsequently, the ions are oxidized to form the desired crystalline phases.

Barium carbonate ($BaCO_3$), strontium carbonate ($SrCO_3$) and ammoniac complex ($NH_4H_2NbO(C_2O_4).3H_2O$) were selected as starting materials. The molar ratio of starting materials was calculated to obtain a final $Sr_{0.75}Ba_{0.25}Nb_2O_6$ (SBN75) phase. For preparation of the resin, $BaCO_3$, $SrCO_3$ and $NH_4H_2NbO(C_2O_4).3H_2O$ were initially dissolved in water to form a transparent solution. Next, each solution was mixed separately with citric acid and heated to 40 °C for 30 minutes. This stage is important to form chelate between mixed cations with a hydroxycarboxylic acid (citric acid). Then, each solution was mixed with ethylene glycol (citric acid/ethylene glycol $= 75/25$) and polymerized by heating up to 100 °C for 30 minutes. Finally, the three solutions were mixed at room temperature and heated again to 50 °C and stirred for 20 minutes to homogenization, when a transparent resin was obtained. The final transparent resin indicates that all metallic ions were distributed throughout the polymeric resin. The viscosity of the final resin was controlled with ethylic alcohol.

Films of the resins were deposited at room temperature on Si and Pt/Si substrates by dip coating. Films were obtained by depositing multiple layers of this resin. Each layer was annealed at 400 °C for one hour, to remove residual solvents. The process was repeated for five deposited layers to obtain a film with 0.5 μm thickness on average. Deposited films were crack-free, uniform and well adhered on both substrates. For crystallization films deposited on Si and Pt/Si substrates were annealed in an electric furnace at 500, 600 and 700 °C for one hour. The rapid thermal crystallization was carried out in a Research INC power controller model 664F rapid thermal annealing (RTA) furnace at 500, 600 and 700 °C for 60 and 120 seconds. The energy source was comprised of several tungsten lamps positioned on the lower side of a

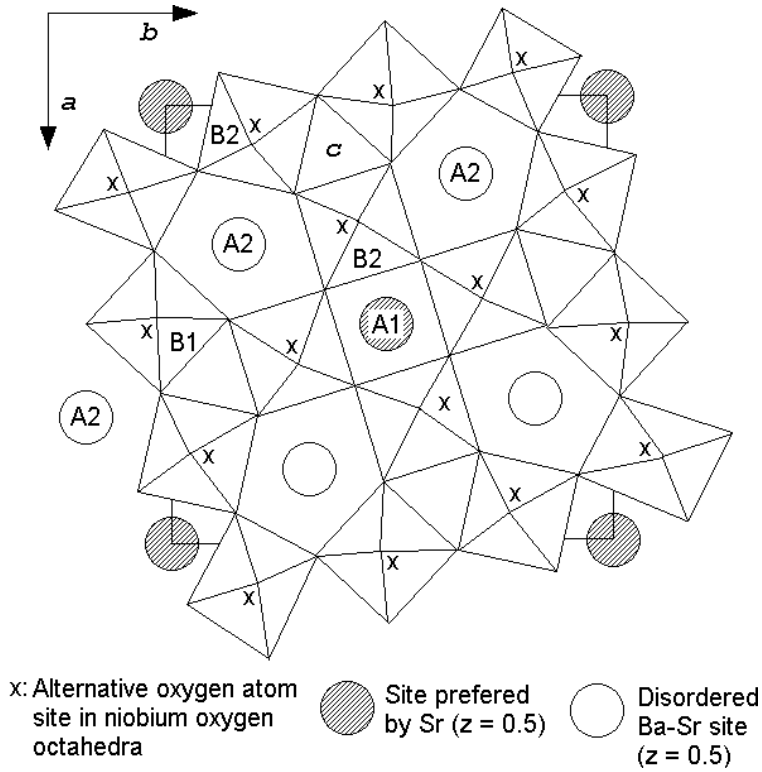

Figure 1. View of strontium barium niobate structure along the polar *c* axis. After Jamieson *et al* [3].

quartz isolation-heating chamber. The structure of the crystallized films at different time and firing temperatures was analysed by x-ray diffraction (XRD) using Cu Kα radiation at room temperature.

3. Results and discussion

In order to study the effect of temperature in SBN crystallization, films were prepared under different conditions. Figure 2 shows XRD patterns of SBN films on Si substrate, heat annealed at 500, 600 and 700 °C for 1 hour using a conventional furnace. Peaks identified in this figure were attributed to tetragonal SBN phase. Some structural fluctuation can be seen in figure 2 for films annealed at 500 °C, when compared with the well defined (001), (311), (002) and (322) peaks. As the annealing temperature was increased, from 500 to 700 °C, these peaks in XRD patterns became sharper and the full width at half maximum decreased, indicating better crystallinity. Based on figure 2, changes of the (001) full width at half maximum (FWHM) film represents the degree of crystallization with annealing temperature. When annealing temperature increases the FWHM of the (001) peak decreases. FWHMs at 500, 600 and 700 °C are 0.66, 0.45 and 0.36°, respectively. This result indicated that SBN film was well crystallized at 700 °C. In figure 2 we can identify the presence of the $SrNb_2O_6$ (SN) and $BaNb_2O_6$ (BN) phases for films annealed at 500 °C for 1 hour. When temperature increases, BN disappears but SN remains in films annealed at 600 and 700 °C for 1 hour. Neither SN

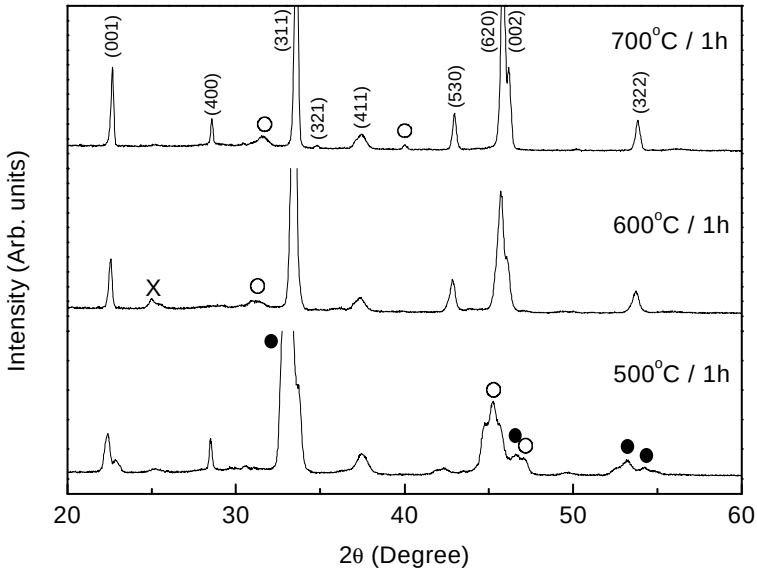

Figure 2. X-ray diffraction patterns of SBN thin films deposited on Si substrate. Films annealed at different temperatures in an electric furnace. Unidentified phase (×), $SrNb_2O_6$ (○) and $BaNb_2O_6$ (●).

nor BN is a ferroelectric material with the tungsten bronze structure. They are components of the solid solution that yields ferroelectric SBN. BN crystallizes in both hexagonal and orthorhombic forms while SN appears to be isostructural with $CaTa_2O_6$ [3].

Figure 3 shows XRD patterns of SBN films on Pt/Si substrate for different temperatures. As we can see, the crystallization process of SBN films on Pt/Si substrate is slightly different if compared with films deposited on Si. As shown in figure 3, polycrystalline SBN phase was only crystallized in films annealed at 600 and 700 °C for 1 hour. The FWHMs of the (001) peak in figure 3 were 0.48 and 0.60° for films respectively annealed at 600 and 700 °C, showing that the film annealed at 600 °C was better crystallized than the film annealed at 700 °C. Undesired SN and BN phases are present in films annealed at 500 °C. As observed in films deposited on Si substrate, the BN phase disappears and only SN remains when the annealing temperature increases from 500 to 700 °C. Figure 3 still shows additional gold (Au) peaks. These electrodes were deposited on top of the films for electrical characterization in future work.

Figure 4 shows XRD patterns of the SBN films in the configuration Au/SBN/Si/Pt, subjected to rapid thermal annealing (RTA), at different annealing temperatures for a constant annealing time of 60 seconds. As indicated by indexed peaks, the SBN phase was just crystallized for film annealed at 700 °C for 60 seconds. The FWHM of the (001) peak was 0.42°, indicating that SBN film was well crystallized at 700 °C for 60 seconds, using RTA. As observed in figure 2 and 3, BN and SN phases are also present in films obtained by the RTA process, but only for films annealed at 500 and 600 °C for 60 seconds. Considering figure 4, SN and BN phases disappear completely when temperature increases up to 700 °C. Finally, figure 5 shows SBN films in the configuration Au/SBN/Si/Pt which were annealed at 700 °C for 60 and 120 seconds. No substantial changes were observed on crystallization of SBN films at different RTA times but small crystallinity fluctuations were suggested by intensity changes in (002) and (620) peaks. For film annealed at 700 °C for 120 seconds the FWHM of the (001) peak was 0.48°, a similar value to the film annealed at 700 °C for 60 seconds. It is important

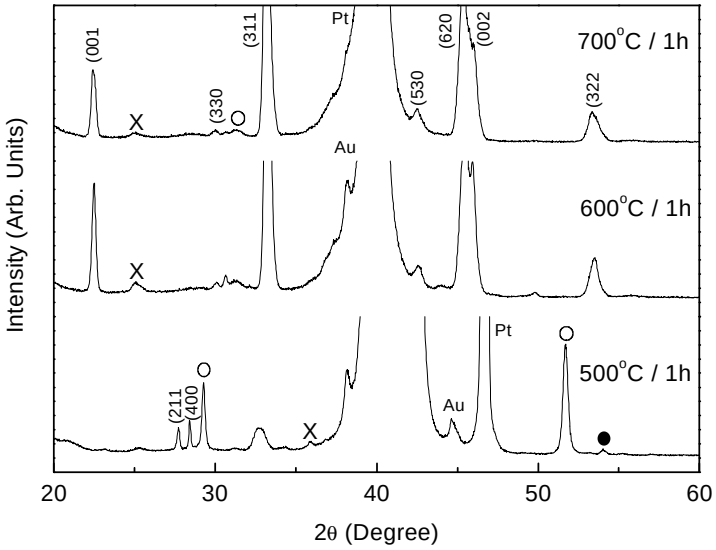

Figure 3. X-ray diffraction patterns of SBN thin films deposited on Pt/Si substrate. Films annealed at different temperatures in an electric furnace. Unidentified phase (×), $SrNb_2O_6$ (○) and $BaNb_2O_6$ (●).

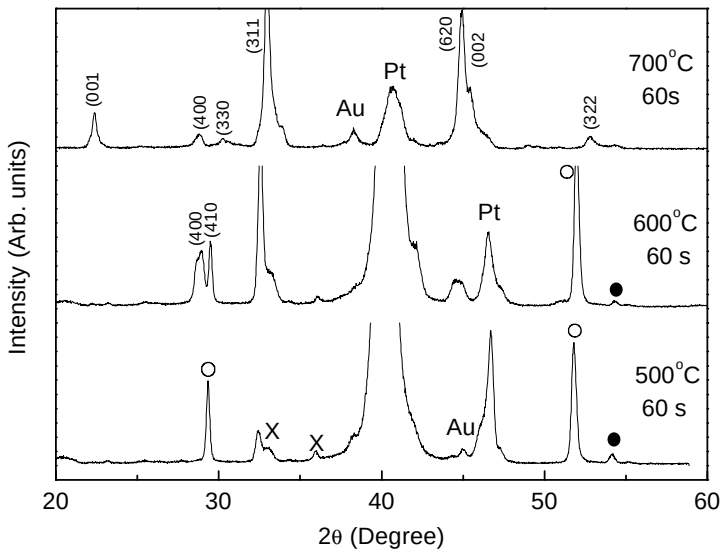

Figure 4. X-ray diffraction patterns of SBN thin films deposited on Pt/Si substrate. Films annealed at different temperatures, using rapid thermal annealing (RTA), for 60 seconds. Unidentified phase (×), $SrNb_2O_6$ (○) and $BaNb_2O_6$ (●).

to note that SN and BN phases disappear for films crystallized at 700 °C using RTA, as may be observed in figures 4 and 5.

Comparing films crystallized at 700 °C, using different methods and substrates, film deposited on Si presented a smaller FWHM, indicating better crystallization for films deposited

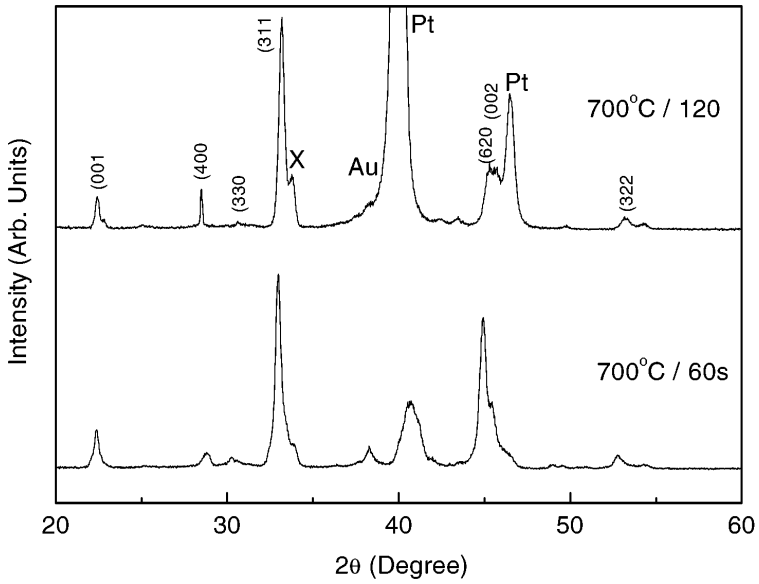

Figure 5. X-ray diffraction patterns of SBN thin films deposited on Pt/Si substrate. Films annealed at 700 °C, using rapid thermal annealing (RTA), for 60 and 120 seconds. Unidentified phase (×).

Table 1. Summary of lattice parameters for tetragonal SBN thin films under different conditions.

	Annealing temperature	Substrate	Lattice constant a (Å)	Lattice constant c (Å)
Conventional furnace	700 °C/1 h	Si	11.426	3.958
	700 °C/1 h	Pt/Si	11.568	3.996
Rapid thermal annealing	700 °C/60 s	Pt/Si	11.625	4.035
	700 °C/120 s	Pt/Si	11.581	4.001

on this substrate. For well crystallized SBN films the lattice constants a and c were calculated for the tetragonal phase using the (001), (311), (002) and (322) peaks from XRD patterns and are summarized in table 1. As shown in this table, the lattice constant changes for different annealing conditions and different substrates. The values obtained of lattice constants a and c ranged from 11.426 to 11.625 Å and 3.958 to 4.035 Å, respectively. Greater values of lattice constant were obtained for films prepared by RTA, deposited on Pt/Si substrate and annealed at 700 °C for 60 seconds. The lattice parameters a and c obtained here agreed relatively well with results of the literature for SBN75 thin film obtained by metallorganic chemical vapour deposition (MOCVD), whose values are around $a = 12.430$ Å and $c = 3.932$ Å [14]. For bulk crystals with same composition the lattice parameters are $a = 12.458$ Å and $c = 3.928$ Å [18]. The slightly smaller a- and greater c-parameters obtained here for SBN films may be attributed to elastic strain generated along the a- and c-axis in SBN films.

There are many works on SBN thin films on different substrates, obtained by several methods. SBN may be preferentially oriented on MgO [10–12] and fused silica substrates [9]. In this last substrate, oriented SBN films can be formed by applying a dc electric field parallel to the surface of the film during the heat treatment. The substrates play important roles for the promotion of crystallization and also for the preferred orientation of films. On MgO(100) substrate, SBN thin films are crystallized in the tetragonal phase with preferred

c-axis orientation and XRD profiles show strong (001) and (002) reflections [10, 11]. On the other hand, SBN thin films crystallized on MgO(111) are polycrystalline without preferential orientation [12]. In the present work SBN films were also polycrystalline with random orientation under different conditions and this result agrees with the literature for SBN films crystallized on silicon substrate [9, 19].

4. Conclusion

In conclusion, polycrystalline SBN thin films of good quality were crystallized on Si and Pt/Si substrates using a polymeric resin. Results showed good crystallization of SBN tetragonal phase when films were annealed at 700 °C for 1 hour on both Si and Pt/Si substrates using a conventional furnace. Films crystallized by the rapid thermal annealing (RTA) method also presented good crystallization. Undesired phases such as $SrNb_2O_6$ and $BaNb_2O_6$ appear in films deposited on Si and Pt/Si substrates for films crystallized using a conventional furnace. Using RTA these phases were eliminated for films annealed at 700 °C for 60 and 120 seconds.

Acknowledgments

The authors are grateful to CNPq and FAPESP (processes 98/16513-5 and 99/02485-2) for financial support and Dr Yvonne P Mascarenhas for XRD facilities.

References

[1] Magneli A 1949 *Ark. Kemi.* **1** 213
[2] Nishiwaki S, Takahashi J, Kodaira K and Kishi M 1996 *Japan. J. Appl. Phys.* **35** 5137
[3] Jamieson P B, Abrahams S C and Bernstein J L 1968 *J. Chem. Phys.* **48** 4352
[4] Trubelja M P, Ryba E and Smith D K 1996 *J. Mater. Sci.* **31** 1435
[5] Glass A M 1969 *J. Appl. Phys.* **40** 4699
[6] Zook J D and Liu S T 1978 *J. Appl. Phys.* **49** 4604
[7] Sakamoto S and Yazaki T 1973 *Appl. Phys. Lett.* **22** 429
[8] Horowitz M, Bekker A and Fischer B 1993 *Appl. Phys. Lett.* **62** 2619
[9] Xu Y, Chen C J, Xu R and Mackenzie J D 1991 *Phys. Rev.* B **44** 35
[10] Hirano S, Yogo T, Kikuta K and Ogiso K 1992 *J. Am. Ceram. Soc.* **75** 1697
[11] Thöny S S, Youden K E, Harris J S Jr and Hesselink L 1994 *Appl. Phys. Lett.* **65** 2018
[12] Guo X L, Liu Z G, Chen X Y, Zhu S N, Xiong S B, Hu W S and Lin C Y 1996 *J. Phys. D: Appl. Phys.* **29** 1632
[13] Nystrom M J, Wessels B W, Lin W P, Wong G K, Neumayer D A and Marks T J 1995 *Appl. Phys. Lett.* **66** 1726
[14] Lee M and Feigelson R S 1997 *J. Cryst. Growth* **180** 220
[15] Mendes R G, Araújo E B, Klein H and Eiras J A 1999 *J. Mater. Sci. Lett.* at press
[16] Pechini M 1967 *US Patent* 3 330 697
[17] Lessing P A 1989 *Ceram. Bull.* **68** 1002
[18] Neurgaonkar R R, Hall W F, Oliver J R, Ho W W and Cory W K 1988 *Ferroelectrics* **87** 167
[19] Chen C J, Xu Y, Xu R and Mackenzie J D 1991 *J. Appl. Phys.* **69** 1763